



# Performance of strength grading methods based on fibre orientation and axial resonance frequency applied to Norway spruce (*Picea abies* L.), Douglas fir (*Pseudotsuga menziesii* (Mirb.) Franco) and European oak (*Quercus petraea* (Matt.) Liebl./*Quercus robur* L.)

Anders Olsson<sup>1</sup> · Guillaume Pot<sup>2</sup> · Joffrey Viguier<sup>2</sup> · Younes Faydi<sup>2</sup> · Jan Oscarsson<sup>1</sup>

Received: 1 June 2018 / Accepted: 13 November 2018 / Published online: 3 December 2018  
© INRA and Springer-Verlag France SAS, part of Springer Nature 2018

## Abstract

• **Key message** Machine strength grading of sawn timber is an important value adding process for the sawmilling industry. By utilizing data of local fibre orientation on timber surfaces, obtained from laser scanning, more accurate prediction of bending strength can be obtained compared to if only axial vibratory measurements are performed. However, the degree of improvement depends on wood species and on board dimensions. It is shown that a model based on a combination of fibre orientation scanning and axial vibratory measurement is very effective for Norway spruce (*Picea abies* L.) and Douglas fir (*Pseudotsuga menziesii* (Mirb.) Franco). For European oak (*Quercus petraea* (Matt.) Liebl./*Quercus robur* L.) boards of narrow dimensions, axial vibratory measurements are ineffective whereas satisfactory results are achieved using a model based on fibre orientation.

• **Context** Machine strength grading of sawn timber is an important value adding process for the sawmilling industry.

• **Aims** The purpose of this paper has been to compare the accuracy of several indicating properties (IPs) to bending strength when applied to Norway spruce (*Picea abies* L.), Douglas fir (*Pseudotsuga menziesii* (Mirb.) Franco) and European oak (*Quercus petraea* (Matt.) Liebl./*Quercus robur* L.).

• **Methods** The IPs were determined for a set of data comprising scanned high-resolution information of fibre orientation on board surfaces, axial resonance frequency, mass and board dimensions.

• **Results** Whereas dynamic axial modulus of elasticity (MoE) gave good prediction of bending strength of Norway spruce ( $R^2 = 0.58$ ) and Douglas fir ( $R^2 = 0.47$ ), it did not for narrow dimension boards of oak ( $R^2 = 0.22$ ). An IP based on fibre orientation gave, however, good prediction of bending strength for all three species and an IP considering both dynamic axial MoE and local fibre orientation for prediction of bending strength gave very good accuracy for all species (Norway spruce  $R^2 = 0.72$ , Douglas fir  $R^2 = 0.62$ , oak  $R^2 = 0.59$ ). Comparisons of results also showed that scanning of fibre orientation on all four sides of boards resulted in more accurate grading compared to when only the two wide faces were scanned.

---

**Handling Editor:** Jean-Michel Leban

**Contribution of the co-authors** The paper is a result of cooperation between two research groups, one in France and one in Sweden which planned and shaped the paper together. Anders Olsson, invited as a guest researcher by the group in France, carried out most of the calculations and writing. Guillaume Pot, who took the initiative to this cooperation, led the work with collection and treatment of experimental data. Joffrey Viguier worked on the treatment of experimental data and produced much of the data of Norway spruce and Douglas fir during its PhD project, just as Younes Faydi did for European oak. Jan Oscarsson contributed with knowledge and background writing on machine strength grading.

✉ Guillaume Pot  
guillaume.pot@ensam.eu

<sup>1</sup> Department of Building Technology, Linnaeus University, SE-351 95 Växjö, Sweden

<sup>2</sup> LaBoMaP, Arts & Métiers, rue Porte de Paris, 71250 Cluny, France

• **Conclusion** Data of local fibre orientation on wood surfaces give basis for accurate machine strength grading. For structural size timber of Norway spruce and Douglas fir, excellent grading accuracy was achieved combining such data with data from vibratory measurements. The improvements achieved enable substantial increase of yield in high-strength classes.

**Keywords** Grain angle · Fibre direction · Tracheid effect · Structural timber · Longitudinal vibrations · Grade determining property

## Abbreviations

MoE	Modulus of elasticity
MC	Moisture content
IP	Indicating property
CoV	Coefficient of variation
$R^2$	Coefficient of determination
SEE	Standard error of estimate
$u$	MC determined according to EN 13183-1 at the time of four point quasi-static bending test
$u_p$	MC determined using pin-type moisture metre at the time of vibrational test
$f$	Resonance frequency of board corresponding to first axial mode of vibration
$\rho$	Average density of board at the time of vibrational test
$\rho_{12\%}$	Average density of board adjusted to 12% MC (adjusted on the basis of $u_p$ )
$E_a$	Axial dynamic MoE of board
$E_{a,12\%}$	$E_a$ adjusted to 12% MC (on the basis of $u_p$ )
$D_{a,12\%}$	Board property corresponding to $E_{a,12\%}$ , but determined disregarding $\rho$
$E_{m,g}$	Global bending MoE, determined by four-point quasi-static bending test
$E_{m,g,12\%}$	$E_{m,g}$ adjusted to 12% MC (on the basis of $u$ )
$f_m$	Bending strength of board, determined by four-point quasi-static bending test
$f_{m,h}$	$f_m$ , adjusted to a reference size, namely board depth, $h$ , of 150 mm
$E_{b,90,nom}$	Lowest bending MoE along board, valid for a moving span of 90 mm, determined on the basis of calculation utilizing data of fibre orientation and nominal values of material parameters
$E_{b,90,nom,2-side}$	$E_{b,90,nom}$ based on data of fibre orientation of two wide faces of board
$E_{b,90,nom,4-side}$	$E_{b,90,nom}$ based on data of fibre orientation of four faces of board
$IP_{E2E}$	IP to $f_{m,h}$ based on linear regression combining $E_{b,90,nom,2-side}$ and $E_{a,12\%}$ as predictor variables

$IP_{E4E}$	IP to $f_{m,h}$ based on linear regression combining $E_{b,90,nom,4-side}$ and $E_{a,12\%}$ as predictor variables
$IP_{E2\rho}$	IP to $f_{m,h}$ based on linear regression combining $E_{b,90,nom,2-side}$ and $\rho_{12\%}$ as predictor variables
$IP_{E2\rho}$	IP to $f_{m,h}$ based on linear regression combining $E_{b,90,nom,4-side}$ and $\rho_{12\%}$ as predictor variables
$IP_{D2\rho}$	IP to $f_{m,h}$ based on linear regression combining $E_{b,90,nom,2-side}$ and $D_{12\%}$ as predictor variables
$IP_{D2\rho}$	IP to $f_{m,h}$ based on linear regression combining $E_{b,90,nom,4-side}$ and $D_{12\%}$ as predictor variables

## 1 Introduction

Effective use of structural timber requires knowledge of properties like stiffness and strength. Major uncertainties of these properties mean that many boards, during grading, are assigned to low-strength classes that do not correspond to their structural potential, which results in poor utilization of the material. Thus, strength grading of sawn timber is an important value adding process for the sawmilling industry. By means of either visual inspection or application of certified grading machines, timber is graded into classes, or grades, for which characteristic values<sup>1</sup> of structural properties are given. In the European Standard EN 338 (2016), a system of strength classes of structural timber to be used in design codes is established for species of both softwood (C-classes) and hardwood (D-classes). According to this standard, timber is graded to a certain strength class on the basis of three so-called *grade determining properties* which are defined in terms of bending strength, modulus of elasticity (MoE) and density. Machine strength grading is based on the statistical relationship between the so-called *indicating properties* (IPs) and each of the three grade determining properties. According to EN 14081-2 (2010), an IP is defined as a measurement, or a

<sup>1</sup> The *characteristic value* of a property is defined such that 95% of the boards assigned to the strength class exceed the characteristic value of the class. Consequently, it is accepted that 5% of the boards have a property value that is below the characteristic value of the class.

combination of measurements, that is made using a grading machine and is closely related to one or more of the grade determining properties.

The first grading machines, which were introduced in Australia (Galligan and McDonald 2000) and in the USA (ALSC 2014) about 1960, were based on IPs reflecting MoE values determined on the basis of bending in the flatwise board direction over span lengths of about 0.9–1.2 m moving along the board. Machines of this type are still in use and the grading is based on the relationship between the lowest flatwise bending MoE found along the board and the edgewise bending strength. This type of machines dominated the market until the 1990s, when strength grading on the basis of axial dynamic excitation was introduced (Görlacher 1990; Ohlsson and Perstorper 1992; Blass and Gard 1994). In this latter technique, an average axial dynamic MoE, here denoted  $E_a$ , of an entire board is used as IP. This MoE value is determined as

$$E_a = 4\rho f^2 L^2 \quad (1)$$

where  $\rho$  is the average density of the board,  $f$  is the resonance frequency of the first axial mode of vibration excited in the board and  $L$  is the board length. Density is often determined on the basis of the board weight which is measured using a scale installed in the production line. In this context, it should be mentioned that there are axial dynamic grading machines in which density information is not utilized, which means that the scale installation is excluded.

Due to simplicity and limited costs, machines based on axial dynamic excitation have today reached a dominating position on the market.

Machine strength grading using the two types of machines described above are, in general, based on grading models in which the prediction of each of the grade determining properties is based on the relationship between one single board property and the grade determining property in question. However, grading machines based on a combination of axial dynamic MoE and X-ray information have been available on the market since the later part of the 1990s. Application of this type of machines imply that density variation within a piece of timber is captured by X-ray scanning and since there is a difference in density between knots and clear wood, the results of this scanning can be used to determine size and position of knots. Different knot measures can then be defined and combined with axial dynamic MoE information into grading models. In general, application of machines based on such models have provided the most accurate strength grading that has been available on the market in recent years (Hanhijärvi and Ranta-Maunus 2008; Olsson 2016). As regards the possibility of using X-rays to identify knots on the basis of difference in density between knots and clear wood (Oh et al. 2009), it should be noted that such density contrasts are generally larger in softwoods than in hardwoods, which implies

that knot detection using X-rays is more useful for softwoods than for hardwoods (Stängle et al. 2015; Viguier 2015).

Ever since the first grading machines based on flatwise bending were introduced, it has been well known that the relationship between bending strength and MoE determined on the basis of bending deformations is dependent on the length over which the deformations are measured (Corder 1965). Over the years, large research efforts have been directed to the determination of MoE corresponding to local bending deformations measured over a few centimetres of a board's length (Kass 1975; Bechtel 1985; Foschi 1987; Boughton 1994). Still, it has been found that the accuracy of MoE values determined on the basis of deformations and loads related to such short spans are often affected by measurement noise and numerical errors (Kass 1975; Foschi 1987). Consequently, no grading method based on measurement of deformations over very short spans has, to the knowledge of the authors, been approved for or applied in commercial machine strength grading.

Regarding the possibility to determine local stiffness with high resolution along boards, and to identify IPs to bending strength based on local bending stiffness, an insight has in recent years been reached regarding the use of fibre orientation data for such purposes (Olsson et al. 2013). Such data is determined using the tracheid effect which is based on the fact that fibres in wood spread concentrated light, such as laser light, better in the longitudinal direction of the fibres than across (Matthews and Beech 1976). Since strength and stiffness properties are far better in the longitudinal fibre direction than in perpendicular directions (Kollman and Côté 1968; Hatayama 1984), even a small angle between fibre direction and longitudinal board direction implies a substantial decrease of local stiffness and strength of a board. Based on information about fibre orientation, axial dynamic MoE, basic material wood properties and cross-sectional integration schemes, a novel IP for bending strength of Norway spruce (*Picea abies* L.) was defined by Olsson et al. (2013) as the lowest calculated local edgewise bending MoE found along the board. An investigation carried out by Olsson and Oscarsson (2017) and comprising more than 900 boards of Norway spruce gave evidence of the performance of the method and this IP. Research aiming at utilization of fibre orientation data for machine strength grading has also been presented by Jehl (2012), Viguier et al. (2015), Viguier et al. (2017) and Lukacevic et al. (2015).

According to the research referred to above, the possibility of determining fibre orientation on board surfaces of softwood species using the tracheid effect is well documented. However, both Zhou and Shen (2003) and Daval et al. (2015) found that this effect is more difficult to discern on hardwoods. As for oak, this was explained by the high density and short length of oak fibres, resulting in an insufficient diffusion of laser light and small size of the laser dot emerging on the board surface.

This paper concerns research regarding to what extent different measured properties may contribute to high accuracy of strength grading of three different wood species. The investigated species were Norway spruce (*Picea abies* L.), Douglas fir (*Pseudotsuga menziesii* (Mirb.) Franco) and European oak (*Quercus petraea* (Matt.) Liebl., *Quercus robur* L.), all of French origin. Since both Norway spruce and Douglas fir are widely used as structural timber in Europe, the need of grading of these species is well understood. As regards hardwoods, it should be noted that from Middle age until the beginning of modern times, oak was the main wood used in France for structural purposes, including production of both buildings and ships (Epaud 2007). Nowadays, oak still represent 33% of French forest land and 26% of the standing volume (IGN 2017). However, in the present era of industrial development, engineered wood products (EWP) such as structural timber, glued laminated timber and cross-laminated timber are developed by softwood since such species are lower in cost because of production processes, growth rate and natural resource prices. Thus, hardwoods are underused since several decades. For instance, the growth of hardwoods in French forest is 54.5 millions m<sup>3</sup>/year whereas only 22 millions m<sup>3</sup>/year are harvested (averaged between 2012 and 2016; IGN 2017).

Prospects of developing the use of hardwood are highlighted in other countries than France. A German National Forest Inventory carried out in 2015 showed that German forests were stocked with approximately 54% coniferous species and 43% hardwood species and that areas with hardwood forests had increased with more than 7% from 2002 to 2012 (Schlotzhauer et al. 2018). This trend is also expected to continue, since new silvicultural approaches in Europe will imply an increase of biodiversity through the creation of mixed forest stands. This development will offer the possibility of a more extensive utilization of hardwoods, including structural purposes.

Thus, the anticipated general increase of hardwood stands in Europe and the large stock of European oak emphasize that the possibility of strength grading oak timber of French origin into strength classes for structural purposes would be of considerable interest for the forestry and sawmilling industries.

The aim of the present paper is to give an overview of the usefulness and relative importance of different types of measured and calculated timber properties employed for strength grading of structural timber of different species, including both softwood and hardwood. Investigated properties are (1) average board density, (2) a measure of axial stiffness based on board length and resonance frequency of the first axial mode of vibration, (3) average axial dynamic modulus of elasticity, (4) local fibre orientation on longitudinal board surfaces, (5) global MoE determined on the basis of four-point bending in accordance with EN 408 (2010) and (6) different combinations of the mentioned properties. As described above, the species investigated were Norway spruce (*Picea*

*abies* L.), Douglas fir (*Pseudotsuga menziesii* (Mirb.) Franco) and European oak (*Quercus robur* L. and *Quercus petraea* (Matt.) Liebl.). The objectives are to present and analyze results in terms of coefficients of determination to bending strength using different IPs that are represented by a single predictor and other IPs that are based on combinations of predictors and application of multiple linear regression.

## 2 Material

In this paper, data from two different experimental studies are included. These earlier studies were focused on machine strength grading of wood species and qualities typically observed in French forests and sawmills. The main species in the first study were Norway spruce (*P. abies*) and Douglas fir (*P. menziesii*), whereas in the second one, European oak (*Q. robur* and *Q. petraea*) was studied. Apart from the species, there are some differences in these two studies that will be detailed in the following, starting from the material in the present section.

### 2.1 Norway spruce and Douglas fir

Data for Norway spruce (*P. abies*) and Douglas fir (*P. menziesii*) was collected in a research project which started in 2012 and finished in 2016. A full account of the background of the project, preparation of material and the laboratory investigations performed are given in Viguier (2015), whereas calculations and evaluations of an IP to bending strength that were developed within the project are presented in Viguier et al. (2017).

Norway spruce trees (*P. abies*) were harvested in Massif Central and Morvan (France). These trees were representative for the usual supply of an industrial sawmill working with a canter line (meaning relatively small diameter logs). The logs were sawn in the same sawmill where the boards were also dried to a mean moisture content (MC) of 11.3%, with a coefficient of variation (CoV) of 13%. Each board was tested with several grading machines and was finally subjected to a destructive mechanical test, as described in Section 3. At the end of this process, data of 437 Norway spruce boards was successfully collected.

Douglas fir (*P. menziesii*) trees were harvested in two regions of France (Massif Central and Pays de la Loire), and the average tree diameter at breast height used to produce the boards was 43 cm (ranging from 29 to 60 cm). The trees were sawn in two different sawmills, with evenly distributed quantities. The same process as described for Norway spruce was applied, resulting in successful collection of full data sets for 805 Douglas fir boards. The mean moisture content was 11.5% (17% CoV).

Both Norway spruce and Douglas fir boards were sawn in three evenly distributed nominal cross sections: 40 ×



100 mm<sup>2</sup>, 50 × 150 mm<sup>2</sup> and 65 × 200 mm<sup>2</sup>. The precise composition of these batches are detailed in Table 1. The length of the boards was about 4 m for all cross sections of both species. It should be noticed that, since the boards were rough sawn, the actual size of each board differed slightly from the nominal size. Thus, the actual dimensions of each board were measured and recorded.

## 2.2 European oak

Data of a sample of European oak came from a second research project, which started in 2014 and finished in 2017. The study is presented in details in Faydi (2017), and a part of the results of the study are published in Faydi et al. (2017). Boards of European oak came from a single sawmill located in the Burgundy region, and which gets its supply from this region. The most prominent species of oak in the region are *Q. petraea* and *Q. robur*. No difference was made between these species concerning mechanical properties since no clear distinction can actually be made between *Q. petraea* and *Q. robur* wood anatomy (Schoch et al. 2004). These species can also hybridize between them and the delimitation between the species is still being debated in literature (Rellstab et al. 2016). The boards of the present sample came directly from the usual production of the sawmill, but mainly boards of the lower qualities of this production were selected, corresponding to the appearance grades QF3 and QF4 according to NF EN 975-1 (2009). This selection was motivated by the fact that these are the qualities that would be considered for used in the construction industry. However, some higher quality boards were included in the sample as well.

The boards were dried to a mean MC of 15.3% (8% CoV). Data of 470 boards was successfully collected and the dimensions were, after planing and cross cut, 22 × 100 × 2000 mm<sup>3</sup> and thus very different in size from those of the Norway spruce and the Douglas fir samples. These dimensions are, however, consistent with typical boards obtained from hardwood sawmills. Since the boards were planed, no subsequent manual or automatic measurements of the board dimensions

**Table 1** Number of boards included of each dimension and each species of the original sample

Size (mm)	Number of pieces		
	Norway spruce ( <i>P. abies</i> )	Douglas fir ( <i>P. menziesii</i> )	European oak ( <i>Q. robur</i> and <i>Q. petraea</i> )
22 × 100 × 2000			470
40 × 100 × 4000	137	235	
50 × 150 × 4000	150	278	
65 × 200 × 4000	150	292	
All sizes	437	805	470

were needed, as it was for the sawn Norway spruce and Douglas fir boards.

## 2.3 Summary of material

The total sample of boards, considered in the present investigation, is summarized in Table 1. Boards included are all those for which data was *successfully collected* in previous investigations. Some boards had then been disregarded of the following reasons; boards broke during manual handling (a few boards of European oak), data that should have been collected during non-destructive assessment was incomplete (some boards of each species) and data that should have been collected during destructive testing was incomplete (some boards of each species).

## 3 Measurements, equipment and collection of data

### 3.1 Determination of weight, moisture content and resonance frequency

In order to obtain the density of each board, the weight and moisture content of every board of every species were measured manually. A scale was used for weighing, and a Gann HT 95 pin-type moisture meter was used to determine the moisture content. To determine the lowest longitudinal resonance frequency, two different devices were used, depending on the two different research projects previously described. However, the principle is the same, based on the *axial dynamic excitation* method mentioned in Section 1 (Eq. 1). It consists in generating an impact with a hammer on a board's end and measuring the resonance frequency of the first axial mode of vibration on either end using a receiver like a microphone or a laser Doppler vibrometer. For the boards of Norway spruce and Douglas fir, several axial dynamic excitation devices were actually used and, not surprisingly, since they are based on the same principle, gave very similar results (Viguier 2015). The data used in the present study come from a handheld device developed for use in industry by Brookhuis (device named Timber Grader MTG). For the oak boards, a manual laboratory device was used, the BING device developed by Brancheriau et al. (2007). This offered, just like its industrial counterpart, an automatic recognition of the resonance frequency.

### 3.2 Determination of local fibre orientation

Two different machines were used to measure local fibre orientation, depending on the research project. However, as for resonance frequency measurements, the physical principle was the same, i.e. in both cases based on the scattering of laser

light, as explained in Section 1. The data recorded from the analysis of an image of laser light on a wood surface was (1) the direction of the major axis of the quasi-elliptical-shaped light spot, which represents the fibre orientation in the plane of the surface, and (2) the *ratio* between the length of the minor and major axes of the light spot.

For boards of Norway spruce and Douglas fir, an industrial scanner from Weinig (CombiScan+) was used. By application of this machine, it was possible to perform measurements on four sides of a board in a single pass. The resolution of the fibre orientation data obtained was 1 mm in the direction along the board and 4 mm in the transversal direction of the board. It is worth noting that because of the rough sawn surface of the Norway spruce and Douglas fir boards, the fibre orientation data was somewhat noisy, as described by Daval et al. (2015).

Figure 1 shows four wood surfaces (a–d) of a 150-mm-long part of one of the Norway spruce boards (the appearance would be similar for a board of Douglas fir)  $50 \times 100$  mm in size, scanned by the industrial scanner. Displayed images show (top row) determined local in-plane fibre orientation of the surfaces and (bottom row) corresponding ratios between the lengths of determined minor and major axes of the quasi-elliptically shaped light spots.

The colour bar to the right provides a basis for interpretation of the images showing this ratio. When the ratio is close to one, which for example happens when a round knot is illuminated, the in-plane component of the fibre orientation is uncertain. Of course, on a round knot, the actual fibre orientation is almost perpendicular to the investigated surface. Therefore, the data from laser scanning was interpreted such that if the ratio between minor and major axes was below 0.8, it was assumed that the fibre orientation coincided with the in-plane orientation that is illustrated in Fig. 1(a). If, on the other hand, the ratio was above 0.8, it was assumed that the fibre orientation was perpendicular to the investigated surface. In the initial research project for which the boards were first prepared and scanned, data of the narrow faces was never used. Within the present investigation, it was discovered that for some boards, data of narrow faces was not properly collected. (The reason was probably strong vibrations of these boards when fed through the scanner.) Therefore, ten boards of the Norway spruce sample, and nine boards of the Douglas fir sample, were discarded for further analysis within the present investigation.

The scanner used for the oak boards was developed in Cluny (France) and was named BobiScan. This is a laboratory scanner

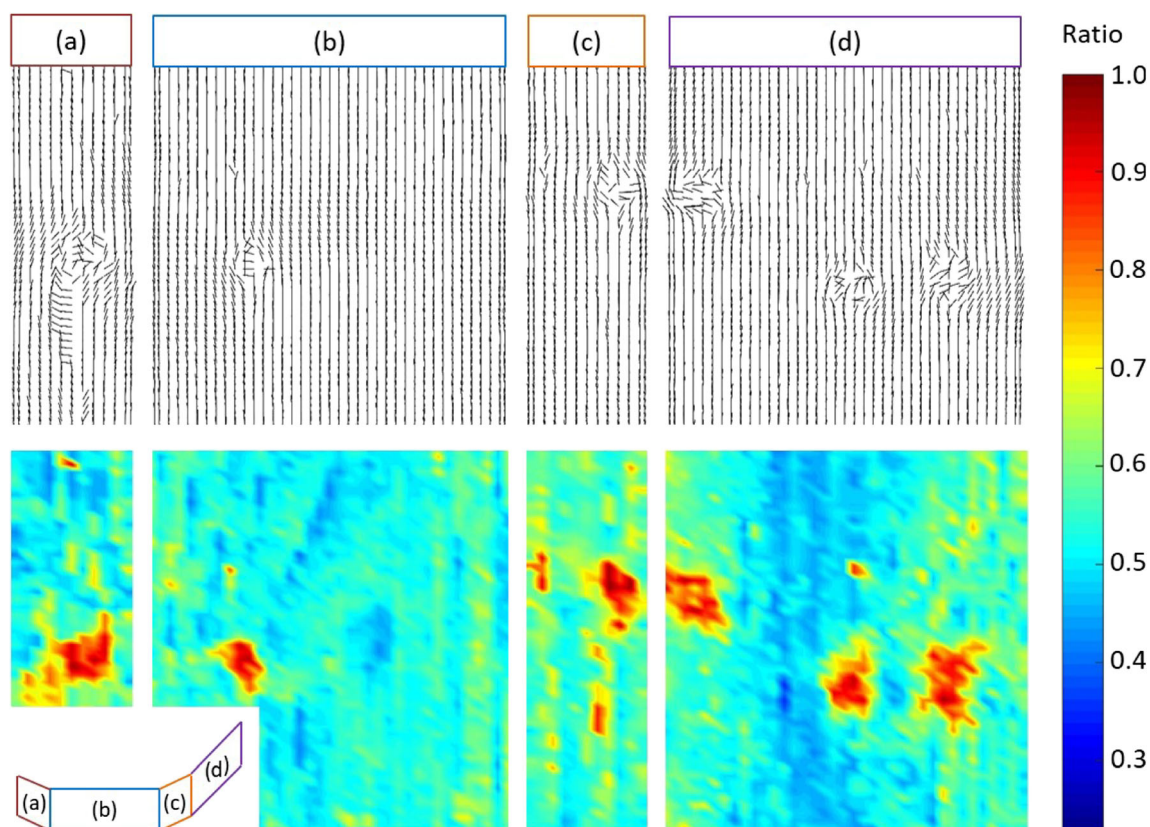


**Fig. 1** Four wood surfaces (a–d) of a 150-mm-long part of a board of Norway spruce,  $50 \times 150$  mm in size. Displayed images show (top row) determined local in-plane fibre orientation of the surfaces and (bottom row) ratios between the determined minor and major axes of elliptically

shaped light spots, all data obtained using an industry scanner. The colour bar to the right provides a basis for interpretation of the colour images that show ratios

by which researchers were able to perform a fine-tuning of the laser, optics and image processing, in a way that would be more difficult using an industry scanner. However, the principle remains the same as its industrial counterpart, based on the tracheid effect. The main difference comes from the wavelength of the lasers which was 1064 nm and their power which could be up to 1 W. Due to these differences, it was possible, using the laboratory scanner, to get good results in terms of laser scattering also for the oak boards. A convincing example of the results is presented in Fig. 2, showing a 120-mm-long part of a board of oak,  $20 \times 100$  mm in size. The experimental setup is schematized Fig. 2(e): two rows of laser dots spaced by 8.8 mm were staggered to obtain a resolution of 4.4 mm in the transversal board direction. A near-infrared camera (Basler acA2000-340kmNIR) was located between the two lasers, and a software was developed to record the individual position of each laser dot while the board was longitudinally moving on a conveyor below the system, resulting in a resolution of 1 mm in the direction along the board. Note that these resolutions are very similar to what was obtained using the industrial scanner used for Norway spruce and Douglas fir. However, in contrast to the industrial scanner, the design of the laboratory scanner implies that only one flat face can be scanned at a time. Furthermore, narrow faces could not be scanned. Thus, every board was scanned twice to obtain the data maps of the two flat faces. Then, on the basis of an image detection of the edges of the board, the data maps of the two large faces were related to a common coordinate system. Regarding

data of ratios between minor and major axes of quasi-elliptically shaped light spots, this was recorded from the laboratory scanner, just as from the industrial scanner, and fibre orientation was determined for oak in the same way as it was for Norway spruce and Douglas fir.

Comparing the in-plane fibre orientation shown in Figs. 1 and 2, respectively, it can be seen that fibre orientation of oak, at some distance from a knot, still deviate from the longitudinal direction of the board, whereas in spruce (and in Douglas fir, although this is not represented in figures), a knot causes fibre deviation only within a shorter distance. Regarding the displayed in-plane components shown in Figs. 1 and 2, note that in order to present clear images, the resolution displayed in the direction along the board is 3 mm, whereas the full resolution obtained from the scanners was actually 1 mm.

### 3.3 Determination of bending strength and global bending MoE

A four-point bending test was performed to assess the bending strength and global bending MoE of the boards. In accordance with EN 408 (2010), the total span between the supports,  $l$ , was set to 18 times the depth of the board,  $h$ . The distance between each point load and the closest support,  $a$ , was set to six times the depth of the board, i.e.  $a = 6h$ , which means that the distance between the two point loads was also  $6h$ .

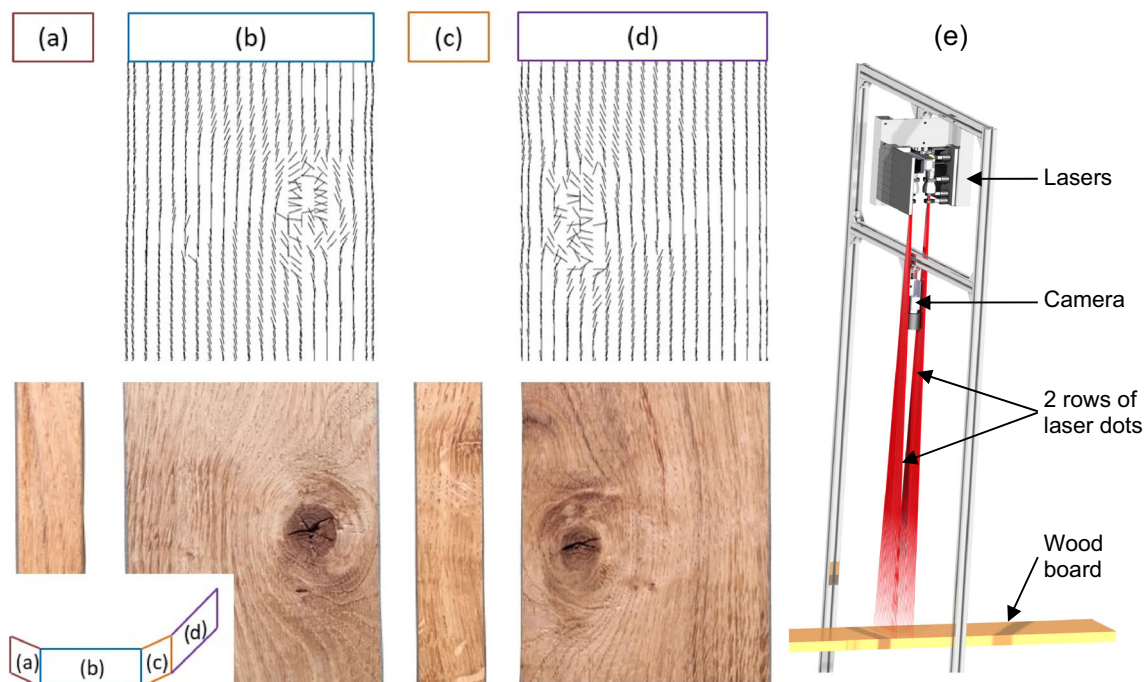


**Fig. 2** Four wood surfaces (a–d) of a 120-mm-long part of a board of oak,  $20 \times 100$  mm in size. Displayed images show (top row) local in-plane fibre orientation of the flat faces obtained using a laboratory scanner and

(bottom row) photographs of the corresponding wood surfaces. Subfigure (e) is a 3D representation of the laboratory scanner used for oak boards



On the basis of the four-point bending test, a global MoE was calculated as

$$E_{m,g} = \frac{3al^2 - 4a^3}{4bh^3 \left( \frac{w_2 - w_1}{F_2 - F_1} - \frac{3a}{5Gbh} \right)} \quad (2)$$

where  $F_1$  and  $F_2$ , respectively, are a lower and a higher level of the total loading applied by the two point loads, and  $w_1$  and  $w_2$ , respectively, are the corresponding global deflection of the mid-point between the point loads.  $G$  represents the shear modulus, here set to infinity. It may be noted that when using  $E_{m,g}$  for calculation of the *grade determining MoE*, used in machine strength grading,  $G$  shall, according to EN 384 (2016) and EN 408 (2010), be set to infinity since shear deformation is included elsewhere in the calculation of the grade determining MoE.

When  $E_{m,g}$  has been determined in accordance with Eq. (2), a correction with respect to MC is performed. According to EN 384 (2016), clause 5.4.2, it shall be done such that the MoE is adjusted with 1% for each percent deviation from 12% MC. Thus, a corrected global bending MoE is calculated as

$$E_{m,g,12\%} = E_{m,g} \left( 1 + \frac{u-12}{100} \right) \quad (3)$$

where  $u$  is the MC in percent determined according to EN 13183-1 (2003) at the time of the bending test.

The bending strength  $f_m$  is calculated in accordance with EN 408 (2010) as

$$f_m = \frac{3F_{\max}a}{bh^2} \quad (4)$$

where  $F_{\max}$  is the maximum value of the total load applied by the two point loads. This bending strength is then corrected for boards with a depth less than 150 mm, i.e. the size effect it taken into account, according to EN 384 (2016), clause 5.4.3 as

$$f_{m,h} = \frac{f_m}{k_h} \quad (5)$$

where

$$k_h = \min \left\{ \left( \frac{150}{h} \right)^{0.2}, 1.3 \right\} \quad (6)$$

In this research, only pieces that broke within the maximum/constant bending zone, i.e. within the point loads, were considered when settings for strength grading was calculated. Thus, all the boards that broke *outside* the point loads, this was about 17% of the total number, were disregarded for further evaluation in the present investigation. The exact

numbers of boards, of each species and size remaining after this, are given in Section 5.

## 4 Definition and determination of indicating properties

In this section, definitions of various IPs to bending strength are given and explained. Single and multiple linear regressions are employed to assess relationships between IPs and bending strength.

### 4.1 Density and axial dynamic modulus of elasticity

The *average board density*, adjusted to an MC of 12% according to EN 384 (2016), was determined as

$$\rho_{12\%} = \frac{m}{L \cdot h \cdot b} \left( 1 - \frac{u_p - 12}{200} \right) \quad (7)$$

where  $u_p$  is the MC in percent determined at the time of the vibrational test using a pin-type moisture metre. In industry, during grading, MC is usually determined using a touch-free moisture metre installed in the production line. The average board density is, of course, a suitable predictor to the *grade determining density* defined in EN 338 (2016) but in commercial machine strength grading, it is usually not used, on its own, as an IP to bending strength. However, in combination with other measures, e.g. when an IP is defined on the basis of multiple linear regression, and thus composed by two or more predictors, it may be suitable for prediction of strength as well. In the present study,  $\rho_{12\%}$  is evaluated both as an IP on its own, and as a predictor included in the definition of other IPs.

The axial *dynamic MoE*, corrected with respect to MC, was calculated on basis of the first axial resonance frequency,  $f$ , as

$$E_{a,12\%} = 4 \frac{m}{L \cdot h \cdot b} \cdot f^2 \cdot L^2 \left( 1 + \frac{u_p - 12}{100} \right) \quad (8)$$

where all variables are defined above.

Finally, an IP which is an equivalent to axial dynamic MoE, except that it is *not* based on knowledge of average board density, is defined as

$$D_{a,12\%} = f^2 \cdot L^2 \left( 1 + \frac{u_p - 12}{100} \right) \quad (9)$$

This IP is often used in commercial machine strength grading, when dynamic excitation machines the use of which do not require weight or density information are employed.



## 4.2 Local bending MoE determined on the basis of fibre orientation

As explained above, wood is an orthotropic material having very high stiffness and strength in the direction along fibres whereas the performance of these properties is much poorer in other directions. As mentioned in Section 1, Olsson et al. (2013) suggested a definition of an IP to bending strength based on knowledge of the in-plane fibre orientation obtained on surfaces, i.e. data that can be obtained as described in Section 2.2. This method was patented (WoodEye 2016) and a full-scale investigation of its performance gave the basis for a formal approval of the methods, and settings for grading of Norway spruce from Sweden, Norway and Finland was presented by Olsson and Oscarsson (2017). In the present research, an IP, very similar to the one suggested and evaluated by Olsson et al. (2013) and Olsson and Oscarsson (2017), is defined and evaluated. The following steps are performed to enable calculation of the IP:

- The fibre orientation, locally on surfaces of the board, are determined from laser scanning.
- It is assumed that the fibre orientation determined on a surface is valid to a certain depth into the board, i.e. that the fibre angle  $\varphi$  highlighted in Fig. 3(a) is assumed to be valid within the volume defined by  $dx \times dA$ .  $dA$  is illustrated in Fig. 3(b1, b2), for the cases when fibre orientation is known on two board surfaces and on four board surfaces, respectively.
- Values of nine independent material parameters of the wood material ( $E$ ,  $G$  and  $\nu$  are MoEs, shear moduli and Poisson's ratios, respectively, and indices  $l$ ,  $r$  and  $t$  refer to longitudinal, radial and tangential direction, respectively), i.e. common values for each of the species investigated, are adopted (see Table 2). On the basis of these, and of each local fibre angle,  $\varphi$ , the corresponding local MoE,  $E_x(x, y, z)$ , valid in longitudinal board direction  $x$  (see Fig. 3(c)), is calculated for every position within the volume of the board (see Olsson et al. 2013 for details of the transformation by which  $E_x(x, y, z)$  is calculated).
- The edgewise bending stiffness for each position  $x$  along the board is calculated by integration over the cross-sectional area as illustrated in Fig. 3(d), i.e. as

$$EI_z(x) = \iint E_x(y-\bar{y})^2 dydz \quad (10)$$

where

$$\bar{y} = \iint E_x y dA / \iint E_x dydz. \quad (11)$$

- A high-resolution bending MoE profile,  $E_b(x)$ , (resolution given by  $dx$ ) is calculated as

$$E_b(x) = \frac{12EI_z(x)}{bh^3} \quad (12)$$

where  $b$  and  $h$ , as above, are the thickness and depth, respectively, of the board cross section. On the basis of the high-resolution MoE profile, a moving average MoE profile, i.e. a more smooth profile of lower resolution, is calculated as

$$\bar{E}_b(x_p, r) = \frac{1}{r} \sum_{x=x_p \pm r/2} E_b(x) dx \quad (13)$$

where  $r$  is the distance (e.g. 0.09 m) over which the moving average is calculated and  $dx$  is the distance (e.g. 0.001 m) between two adjacent positions, in direction along the board, where fibre angles are detected. The graph shown in Fig. 3(e) is  $\bar{E}_b(x_p, r = 0.090)$  of one board.

On the basis of the method explained, an IP to bending strength is now defined. This represents the lowest value of the calculated 90 mm moving average MoE profile, i.e.

$$E_{b,90,nom} = \frac{1}{0.090} \min_{p_1 < x_p < p_2} \left( \sum_{x=x_p \pm 0.045} E_b(x) dx \right) \quad (14)$$

where  $p_1$  and  $p_2$ , respectively, are the positions between which the MoE profile of the board is considered. In actual grading,  $p_1$  and  $p_2$  should be the positions of the ends of the board, except for a necessary margin of 45 mm at each end, i.e. then  $p_2 - p_1 = L - 0.090$ . However, herein  $p_1$  and  $p_2$  are set to the positions where the two point loads are applied in the four-point bending test, i.e.  $p_2 - p_1 = 6h$ . This is to enable a fair and accurate comparison of the accuracy when assessing boards of the different species, since boards of different length were used for the different species. Regarding the notation *nom* of the index of  $E_{b,90,nom}$  this is used to indicate that the calculation is based on *nominal* values of the material parameters, i.e. that values given in Table 2 are used for each board of a certain species. In contrast to this, Olsson et al. (2013) included knowledge of a board-specific MoE, namely  $E_{a,12\%}$ , in the calculation of the IP. Finally, note that the calculated  $E_{b,90,nom}$  may be based on knowledge of fibre orientation of *two sides* of the board, as illustrated in Fig. 3(b1), or of *four sides*, as illustrated in Fig. 3(b2). Consequently, the IP is denoted  $E_{b,90,nom,2-side}$  when fibre orientation data of two sides of the board are utilized, and  $E_{b,90,nom,4-side}$ , when fibre orientation data of four sides of the board are utilized.

Regarding the values of nominal material parameters given in Table 2, note that what actually matters for the present purpose is the *relationship* between parameters, e.g. the relationship between  $E_l$  and  $E_t$  of a species, rather than if the whole set of values, i.e. all MoEs and shear moduli of the species, is high or low. It should also be mentioned that the parameters given for oak in Table 2 were actually determined for red oak (*Quercus rubra*)

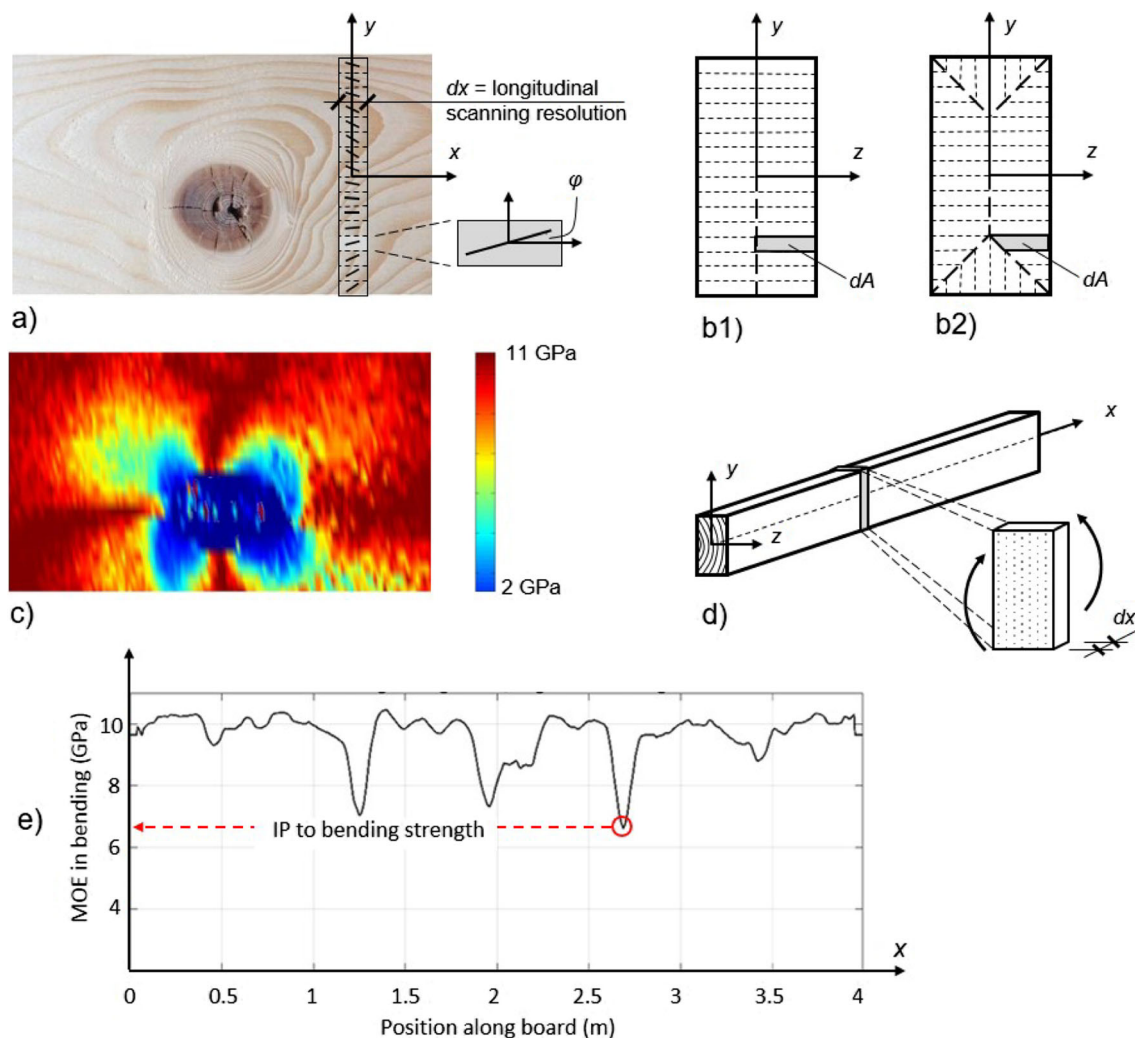


**Fig. 3** (a) Local fibre orientation scanned on a member's surface by means of a row of laser dots, (b1, b2) cross-section divided into sub-areas implying that the exhibited angle  $\varphi$  and corresponding MoE in the longitudinal direction,  $E_x(x,y,z)$ , are valid within the volume  $dA \times dx$  (b1, b2 represent, respectively, the case when fibre angles are detected on

two sides and on four sides of the board), (c) distribution of longitudinal MoE around the exhibited knot, (d) segment of length  $dx$  for which the edgewise bending stiffness is calculated by integration over its cross section, and (e) a bending MoE profile obtained by considering all the segments of the board (Fig. 3a,c from Oscarsson et al. 2014)

(Guitard 1987). However, this has no practical significance since the relationships between the material parameters for these oak species are considered to be similar which is explained by their similar microstructure.

### 4.3 Indicating properties based on multiple linear regression

Multiple linear regression means that two or more basic variables, predictors, are used to establish the linear function that gives the highest coefficient of determination to the dependent variable, which in this case is  $f_{m,h}$ . Thus, if multiple linear regression is performed for the case when, e.g.  $E_{b,90,nom,2-side}$  and  $E_{a,12\%}$  are included as predictors, the IP to the dependent variable  $f_{m,h}$  is established as

$$IP_{E2E}(E_{b,90,nom,2-side}, E_{dyn,12}) = k_0 + k_1 \cdot E_{b,90,nom,2-side} + k_2 \cdot E_{dyn,12} \quad (15)$$

where  $k_1$  and  $k_2$  are assigned the numbers that give the highest possible coefficient of determination between  $IP_{E2E}(E_{b,90,nom,2-side}, E_{a,12\%})$  and  $f_{m,h}$  of the sample, and  $k_0$  is assigned the value that makes the line of regression go through the origin. In this research, six different IPs are established by means of multiple linear regression. Each of these is composed of two of the IPs/predictors defined in Sections 3.1–3.2. The notations used, and the predictors involved in each of the composed IPs, are given in Table 3.

**Table 2** Nominal wood material parameters ( $E$ ,  $G$  and  $\nu$  are MoEs, shear moduli and Poisson’s ratios, respectively, and indices  $l$ ,  $r$  and  $t$  refer to longitudinal, radial and tangential direction, respectively) of three species; values for Norway spruce originate from Dinwoodie (2000), and values for Douglas fir and oak originate from Guitard (1987)

	Norway spruce	Douglas fir	European oak	
$E_l$	10,700	16,400	14,800	MPa
$E_r$	710	1300	1500	MPa
$E_t$	430	900	828	MPa
$G_{lr}$	500	1180	967	MPa
$G_{lt}$	620	910	695	MPa
$G_{rt}$	24	79	398	MPa
$\nu_{lr}$	0.38	0.43	0.59	
$\nu_{lt}$	0.51	0.37	0.69	
$\nu_{rt}$	0.51	0.63	0.54	

### 5 Results

In Table 4, calculated mean values (mean) and coefficients of variation (CoV) of corrected bending strength ( $f_{m,h}$ ), corrected global bending MoE ( $E_{m,g,12\%}$ ), corrected board density ( $\rho_{12\%}$ ), moisture content determined according to EN 13183-1 ( $u$ ) and corrected axial dynamic MoE ( $E_{a,12\%}$ ) are presented for all three species included in the investigation. Mean and CoV are presented separately for each species and each size, and together for all sizes of each species. For seven oak boards, the MC exceeded 18%. Yet,  $E_{m,g,12\%}$  and the IPs of these board were corrected with respect to MC as all the other boards were, i.e. according to Eqs. (7–9) (according to EN 384 2016, correction with respect to MC shall only be done up to 18% MC). It appears from this table that the adjusted strength of European oak is significantly higher than that of Douglas fir and Norway spruce (47.3 MPa against 34.7 MPa and 31.8 MPa, respectively), while its adjusted global MoE is quite similar to that of Douglas fir (10.8 GPa and 10.4 GPa, respectively) and higher than that of Norway spruce (8.82 GPa). The coefficients of variation of these two parameters are, however, higher for European oak. Moreover, no clear difference appears between the different cross sections of a given species.

**Table 3** Notations and predictors of IPs defined using multiple linear regression

Notation of IP	Short notation	Predictors involved
$IP_{E2E}$ ( $E_{b,90,nom,2-side}$ , $E_{a,12\%}$ )	$IP_{E2E}$	$E_{b,90,nom,2-side}$ $E_{a,12\%}$
$IP_{E4E}$ ( $E_{b,90,nom,4-side}$ , $E_{a,12\%}$ )	$IP_{E4E}$	$E_{b,90,nom,4-side}$ $E_{a,12\%}$
$IP_{E2\rho}$ ( $E_{b,90,nom,2-side}$ , $\rho_{12\%}$ )	$IP_{E2\rho}$	$E_{b,90,nom,2-side}$ $\rho_{12\%}$
$IP_{E4\rho}$ ( $E_{b,90,nom,4-side}$ , $\rho_{12\%}$ )	$IP_{E4\rho}$	$E_{b,90,nom,4-side}$ $\rho_{12\%}$
$IP_{E2D}$ ( $E_{b,90,nom,2-side}$ , $D_{a,12\%}$ )	$IP_{E2D}$	$E_{b,90,nom,2-side}$ $D_{a,12\%}$
$IP_{E4D}$ ( $E_{b,90,nom,4-side}$ , $D_{a,12\%}$ )	$IP_{E4D}$	$E_{b,90,nom,4-side}$ $D_{a,12\%}$

In Fig. 4, detailed results are displayed for one board of each species. For boards of (a) Norway spruce, (b) Douglas fir and (c) European oak, calculated local MoE in longitudinal board direction is visualized by colour plots where red colour represents a local MoE =  $E_l$ , meaning that the fibre orientation in such areas is close to being parallel with the longitudinal direction of the board, and blue colour represents MoE =  $E_t$ , meaning that the orientation of the fibres is close to being perpendicular to the longitudinal board direction. Graphs drawn below each colour map show calculated bending MoE profiles, where vertical blue lines indicate positions of point loads in four-point bending tests, and horizontal red arrows indicate values of (a, b)  $E_{b,90,nom,4-side}$  and (c)  $E_{b,90,nom,2-side}$ .

Coefficients of determination ( $R^2$ ) to  $f_{m,h}$  of the different IPs defined in Section 3.3 are presented in Table 5. Coefficients of determination are presented separately for each species and size, and together for all sizes of each species. For some coefficients of determination, a 95% confidence interval is given as well (numbers in parenthesis). The range of the calculated confidence intervals depend on the coefficient of determination, on the size of the sample and on the number of predictors used, i.e. one or two. For comparison,  $R^2$  between  $E_{m,g,12\%}$  and  $f_{m,h}$  is also included in Table 5, even though  $E_{m,g,12\%}$  is determined during destructive testing and not an IP that would actually be used for strength grading.

In Fig. 5a, c, e are shown scatterplots of the relationship between  $E_{a,12\%}$  and  $f_{m,h}$ , for Norway spruce, Douglas fir and oak, respectively, all sizes of each species included in the scatter plots. In Fig. 5b, d are shown scatterplots of the relationship between  $IP_{E4E}$  and  $f_{m,h}$ , for Norway spruce and Douglas fir, respectively, and in Fig. 5e is shown a scatterplot of the relationship between  $IP_{E2E}$  and  $f_{m,h}$  (note that  $IP_{E4E}$  is not available for oak, since only the wide faces of the oak boards were scanned). In connection with each of the scatterplots, the coefficient of determination, the standard errors of estimate (SEE) and the regression equation are given as well.

### 6 Discussion

#### 6.1 Single predictors based on local fibre orientation

In Fig. 4, colour maps representative of the MoE in longitudinal board direction are presented for one board of each species. Since the IPs  $E_{b,90,nom,2-side}$  and  $E_{b,90,nom,4-side}$  are computed from this data, typical differences between the boards should be discussed. In most cases, knots in Douglas fir are larger than those in Norway spruce. However, exceptions are common. The corresponding colour maps of several other Norway spruce boards investigated in this research actually look similar to the board of Douglas fir displayed in Fig. 4b.

**Table 4** Mean values and coefficients of variation of corrected bending strength, corrected global bending MoE, corrected board density, moisture content and corrected dynamic axial MoE

Sample		$f_{m,h}$		$E_{m,g,12\%}$		$\rho_{12\%}$		$u$		$E_{a,12\%}$	
		Mean [MPa]	CoV [%]	Mean [GPa]	CoV [%]	Mean [kg/m <sup>3</sup> ]	CoV [%]	Mean [%]	CoV [%]	Mean [GPa]	CoV [%]
Spruce	40 × 100 (123 pieces)	32.9	36.0	9.35	21.1	451	12.2	12.0	10.2	10.1	20.7
	50 × 150 (128 pieces)	33.4	37.3	9.23	22.6	430	9.4	10.0	12.6	9.83	23.1
	65 × 200 (115 pieces)	28.8	31.9	7.81	18.3	396	8.4	11.9	7.1	8.42	20.0
	All sizes (366 pieces)	31.8	36.1	8.82	22.4	426	11.6	11.3	13.0	9.47	22.8
Douglas	40 × 100 (212 pieces)	33.5	32.5	10.0	16.7	475	6.5	11.2	19.2	10.7	18.0
	50 × 150 (236 pieces)	34.0	34.0	10.3	18.3	483	8.0	11.5	12.9	10.9	18.8
	65 × 200 (237 pieces)	36.5	34.0	10.9	17.9	500	9.1	11.9	12.2	11.4	18.1
	All sizes (685 pieces)	34.7	33.9	10.4	18.0	486	8.3	11.6	15.0	11.0	18.5
Oak	22 × 100 (357 pieces)	47.3	43.8	10.8	27.5	758	6.8	15.3	7.7	12.2	23.9

Correspondingly, colour maps of some of the investigated Douglas fir boards look similar to the one displayed for the Norway spruce board. Regarding oak, knots are often big and cause substantial fibre distortion that can easily affect the entire cross section of narrow dimension boards. This can be seen in Fig. 4c, in which two positions along this board are blue over almost the entire board cross section.

For Norway spruce  $R^2$  to  $f_{m,h}$  is, for  $E_{b,90,nom,2-side}$  and  $E_{b,90,nom,4-side}$ , 0.46 and 0.49, respectively. For Douglas fir, it is 0.35 and 0.43, respectively. For the oak sample,  $E_{b,90,nom,2-side}$  is a good predictor to  $f_{m,h}$ , with a higher value ( $R^2 = 0.56$ ) than for Norway spruce and Douglas fir. This is explained by the fact that oak present larger areas of disturbed fibre orientation around knots, than what is the case for Norway spruce or Douglas fir which present smaller knots and groups of several knots in clusters (as shown in Fig. 4). As a result, the mechanical model based on knowledge of local fibre orientation may be even more effective on oak, because here local weakness is (1) more pronounced and (2) often represented by a single big knot and corresponding fibre distortion. Hu (2018) showed that bending MoE profiles, calculated according to Eqs. (10–14), represent the local compliance to bending more accurately for single big knots than what it does for clusters of smaller knots. In addition, the boards of the oak sample were thinner (22 mm), which may also contribute to good performance of the model, which is based on data of surface scanning.

## 6.2 Global single predictors

As shown in Table 5,  $E_{a,12\%}$  is, for the Norway spruce sample, the single predictor (except  $E_{m,g,12\%}$ ) that gives

the highest coefficient of determination to  $f_{m,h}$ ,  $R^2 = 0.58$ . This is higher than the corresponding coefficient of determination using  $E_{b,90,nom,4-side}$ . Using  $\rho_{12\%}$  and  $D_{a,12\%}$  as IPs gives  $R^2 = 0.30$  and  $R^2 = 0.47$ , respectively. These coefficients of determination are rather high compared to what have been reported in other studies (e.g. Hanhijärvi and Ranta-Maunus 2008; Olsson et al. 2013; Olsson and Oscarsson 2017). The corresponding relationships of the total sample of Douglas fir, i.e. the performance of  $E_{a,12\%}$ ,  $\rho_{12\%}$  and  $D_{a,12\%}$  are  $R^2 = 0.47$ , 0.25 and 0.38, respectively. Thus,  $E_{a,12\%}$  enables a fair prediction of bending strength of Douglas fir. For the European oak sample, however,  $E_{a,12\%}$  gives poor basis for strength grading since, for this sample,  $R^2$  between  $E_{a,12\%}$  and  $f_{m,h}$  is as low as 0.22. The relationship between  $\rho_{12\%}$  and  $f_{m,h}$  for the oak sample is also extremely low,  $R^2 = 0.03$ . Both of these results are consistent with findings of Faydi et al. (2017) who conducted a study on dynamic properties of oak.

Regarding oak, the poor relationship between strength and the global single predictors is explained by the fact that whereas bending strength of boards containing single large knots become very low, single large knots may still have limited effect on  $E_{a,12\%}$ ,  $\rho_{12\%}$  or  $D_{a,12\%}$ . Of course, effects related to large knots should be particularly strong for oak boards of narrow dimensions, since the entire cross section of such boards may be affected by a single knot and the corresponding fibre distortion. The influence on  $E_{a,12\%}$  of a big knot is also dependent on where along the board the knot is located, since the first axial resonance frequency is more or less affected by a local weak section depending on



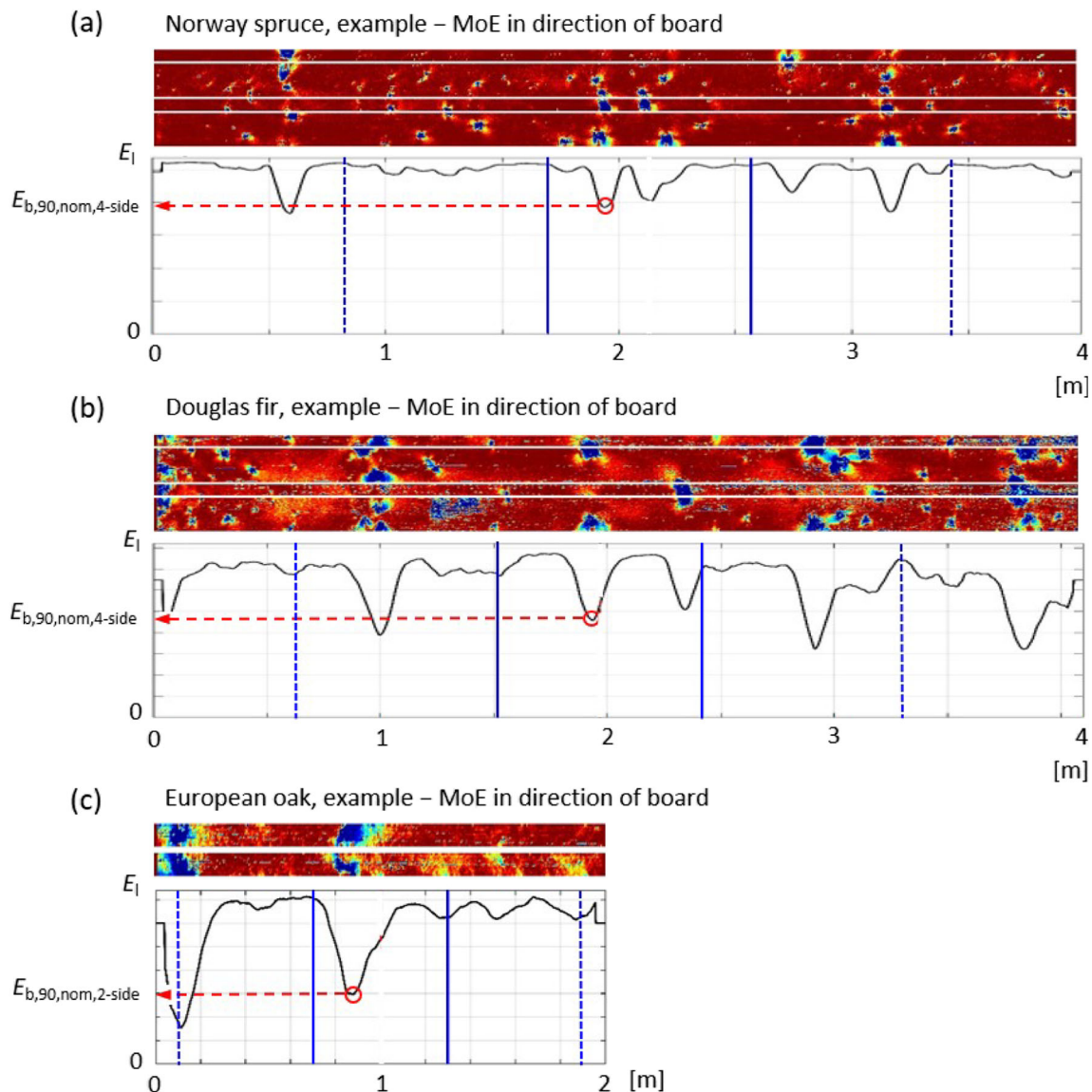


**Fig. 4** For one board of each species—calculated MoE in longitudinal board direction visualized by colour plots (of four and two sides of boards, respectively) where red colour represents  $\text{MoE} = E_l$  (i.e. high MoE, fibre orientation close to parallel with longitudinal board direction) and blue colour represents  $\text{MoE} = E_t$  (i.e. low MoE, fibre orientation close to perpendicular to longitudinal board direction). Graphs drawn below

each colour map show calculated bending MoE profiles,  $E_{b,90,nom}(x)$  where vertical solid and dashed blue lines indicate positions of point loads and positions of supports, respectively, of four-point bending tests, and horizontal red arrows indicate values of **a**, **b**  $E_{b,90,nom,4-side}$  for Norway spruce and Douglas fir and **c**  $E_{b,90,nom,2-side}$  for European oak

where it is located in longitudinal direction. The scatterplot displayed in Fig. 5e shows the relationship between  $E_{a,12\%}$  and  $f_{m,h}$  for the oak sample and this strengthens the presented explanation of the low coefficient of determination between  $E_{a,12\%}$  and  $f_{m,h}$ . There is, clearly, a positive although not very strong correlation between  $E_{a,12\%}$  and  $f_{m,h}$  for the majority of the boards but there are also several boards with quite high values of  $E_{a,12\%}$  but very low values of  $f_{m,h}$ . Regarding the Norway spruce sample and the Douglas fir sample, there are not equally clear indications of this effect, i.e. that  $E_{a,12\%}$ ,  $\rho_{12\%}$  and  $D_{a,12\%}$  would be less accurate for prediction of  $f_{m,h}$  for small size boards

compared to what they are for large boards. However, the small size board of these samples, i.e.  $40 \times 100$  mm, is not a very narrow dimension in comparison with the typical size of knot in these species, especially not for Norway spruce. For Douglas fir, the coefficient of determination between, for example,  $E_{a,12\%}$  and  $f_{m,h}$  is lower ( $R^2 = 0.37$ ) for boards of size  $40 \times 100$  mm than what it is for boards of size  $50 \times 150$  mm and  $65 \times 200$  mm (which is  $R^2 = 0.49$  and  $R^2 = 0.51$ , respectively). However, since the 95% confidence intervals for each of these numbers are about  $\pm 0.09$ , there is no clear evidence of this kind of size effect for the Douglas fir boards.

**Table 5** Coefficients of determination between IPs and corrected bending strength. Numbers given in parenthesis give a 95% confidence interval of the corresponding coefficients of determination

IP	$f_{m,h}$								
	Spruce				Douglas fir				Oak
	40 × 100	50 × 150	65 × 200	All dim.	40 × 100	50 × 150	65 × 200	All dim.	22 × 100
$E_{m,g,12\%}$	0.64	0.76	0.65	0.69 (±0.05)	0.51	0.60	0.60	0.58 (±0.05)	0.53 (±0.05)
$E_{a,12\%}$	0.54 (±0.12)	0.66 (±0.09)	0.49 (±0.13)	0.58 (±0.07)	0.37 (±0.10)	0.49 (±0.09)	0.51 (±0.09)	0.47 (±0.05)	0.22 (±0.08)
$\rho_{12\%}$	0.38	0.29	0.18	0.30 (±0.08)	0.16	0.25	0.29	0.25 (±0.06)	0.03 (±0.03)
$D_{a,12\%}$	0.28	0.59	0.50	0.47 (±0.07)	0.33	0.43	0.40	0.38 (±0.06)	0.17 (±0.07)
$E_{b,90,nom,2-side}$	0.48	0.46	0.41	0.46 (±0.07)	0.30	0.43	0.38	0.35 (±0.06)	0.56 (±0.07)
$E_{b,90,nom,4-side}$	0.45	0.56	0.47	0.49 (±0.07)	0.31	0.48	0.51	0.43 (±0.06)	
$IP_{E2E}$ ( $E_{b,90,nom,2-side}$ , $E_{a,12\%}$ )	0.67	0.75	0.62	0.69 (±0.05)	0.50	0.64	0.58	0.57 (±0.05)	0.59 (±0.06)
$IP_{E4E}$ ( $E_{b,90,nom,4-side}$ , $E_{a,12\%}$ )	0.68 (±0.09)	0.77 (±0.07)	0.67 (±0.10)	0.72 (±0.05)	0.51 (±0.09)	0.66 (±0.07)	0.65 (±0.07)	0.62 (±0.04)	
$IP_{E2\rho}$ ( $E_{b,90,nom,2-side}$ , $\rho_{12\%}$ )	0.64	0.66	0.56	0.61 (±0.06)	0.41	0.57	0.53	0.51 (±0.05)	0.59 (±0.06)
$IP_{E4\rho}$ ( $E_{b,90,nom,4-side}$ , $\rho_{12\%}$ )	0.63	0.68	0.62	0.64 (±0.06)	0.40	0.61	0.63	0.56 (±0.05)	
$IP_{E2D}$ ( $E_{b,90,nom,2-side}$ , $D_{a,12\%}$ )	0.54	0.65	0.57	0.58 (±0.06)	0.47	0.58	0.48	0.49 (±0.05)	0.57 (±0.07)
$IP_{E4D}$ ( $E_{b,90,nom,4-side}$ , $D_{a,12\%}$ )	0.53	0.69	0.62	0.62 (±0.06)	0.48	0.60	0.57	0.55 (±0.05)	

### 6.3 Indicating properties based on multiple linear regression

The predictors  $E_{a,12\%}$ ,  $\rho_{12\%}$  and  $D_{a,12\%}$  are measures of global board properties whereas  $E_{b,90,nom,2-side}$  and  $E_{b,90,nom,4-side}$  are based on local fibre orientation. Therefore, it should be fruitful to combine one predictor of each kind by means of multiple linear regression as is done herein, and the results presented in Table 5 confirm that this is successful. The highest coefficient of determination to  $f_{m,h}$  is obtained using  $IP_{E4E}$ , giving  $R^2 = 0.72$  and  $R^2 = 0.62$  for the Norway spruce and Douglas fir samples, respectively (to be compared to  $R^2 = 0.58$  and  $R^2 = 0.47$ , respectively, using  $E_{a,12\%}$  as IP). This means a substantial improvement with respect to grading accuracy, and the result for the Norway spruce sample is in close agreement with what has been reported for Norway spruce from Sweden, Norway and Finland using similar IPs (Olsson and Oscarsson 2017). The coefficient of determination between IPs and  $f_{m,h}$  obtained for the Norway spruce sample is higher than what it is for the Douglas fir sample but the improvement using  $IP_{E4E}$  rather than  $E_{a,12\%}$  for prediction of  $f_{m,h}$  is comparable for the two species. The IPs  $IP_{E4\rho}$  and  $IP_{E4D}$ , which are established without knowledge of resonance frequency and density, respectively, gave coefficient of determination to  $f_{m,h}$  of  $R^2 = 0.64$  and  $R^2 = 0.62$ , respectively, for the Norway spruce sample. Thus, these IPs do not enable as accurate grading as what  $IP_{E4E}$  does but they give more accurate grading

than what can be obtained using e.g.  $E_{a,12\%}$  alone. As expected,  $IP_{E4E}$  gives higher  $R^2$  to  $f_{m,h}$  than what  $IP_{E2E}$  does (the latter IP based on laser scanning of two faces of the board rather than on four faces). Coefficient of determination obtained for  $IP_{E4E}$  and  $IP_{E2E}$  is, for the Norway spruce sample,  $R^2 = 0.72$  and  $R^2 = 0.69$ , respectively. For the Douglas fir sample, the corresponding numbers are  $R^2 = 0.62$  and  $R^2 = 0.57$ , respectively. Both for Norway spruce and for Douglas fir, the improvement of using  $IP_{E4E}$  rather than  $IP_{E2E}$  is more pronounced for large dimension boards (thick boards) than what it is for narrow dimension boards. For the oak sample, rather limited improvements in grading accuracy are obtained when using  $IP_{E2E}$ ,  $IP_{E2\rho}$  or  $IP_{E2D}$ , rather than the single predictor  $E_{b,90,nom,2-side}$ , for prediction of  $f_{m,h}$ .

### 6.4 Significance of improved grading accuracy on yield in production

As explained in the Section 1, there are different grade determining properties, namely bending strength, modulus of elasticity and density, and the accuracy by which these properties are predicted, is decisive for the yield in different strength classes. Bending strength is the most difficult property to predict and the accuracy obtained in this respect is often crucial for the performance of the grading method in terms of the yield in different strength classes, given a certain quality of the raw material. This is the reason why the current paper

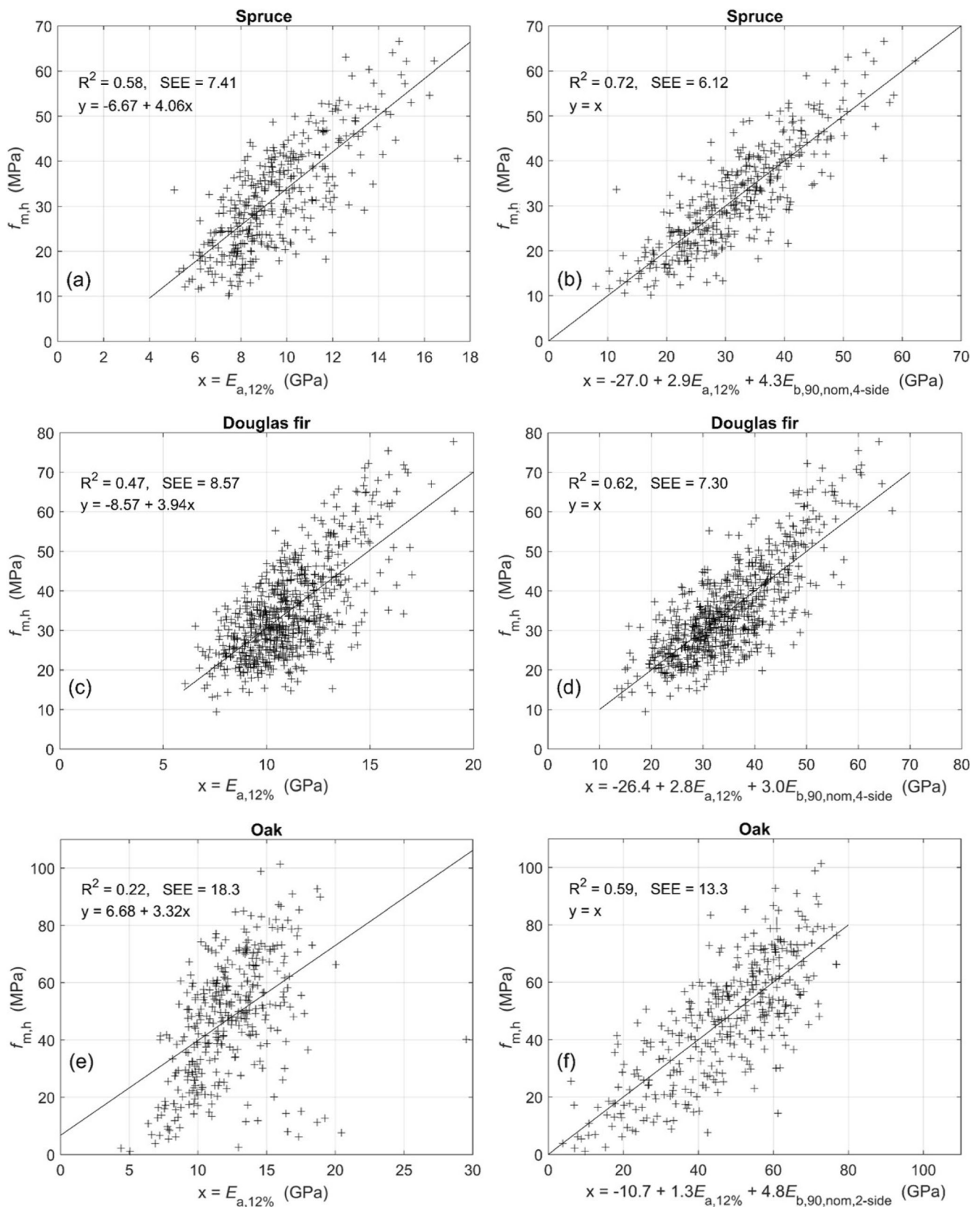


**Fig. 5** Scatterplots of relationship between  $E_{a,12\%}$  and  $f_{m,h}$ , for **a** Norway spruce, **c** Douglas fir and **e** oak. Scatterplots of the relationship between  $IP_{E4E}$  and  $f_{m,h}$  for **b** Norway spruce and **d** Douglas fir, and **e** scatterplot of

the relationship between  $IP_{E2E}$  and  $f_{m,h}$  for oak. Presented in connection to each scatterplot are coefficient of determination, standard errors of estimate (SEE) and regression equation,  $y(x)$

focuses on prediction of bending strength. The rules laid down in the standard EN 14081-2 (2010) on how to calculate the yield in strength classes are, however, rather complicated and it is beyond the scope of this paper to give an account of these rules and to present results in terms of yield in different strength classes using the different IPs defined herein. Yet, a short discussion of the relationship between, on one hand, coefficient of determination (i.e.  $R^2$  between different IPs and  $f_{m,h}$ ) and, on the other hand, yield in strength classes follows. Results presented in earlier studies (Hoffmeyer 1995; Olsson and Oscarsson 2017; Viguier et al. 2017) show that an improvement of the coefficient of determination between IP and  $f_{m,h}$ , from say 0.5 to 0.6, or from 0.6 to 0.7, corresponds to a considerable increase of yield in high-strength classes (e.g. C35), but only to minor improvement in the yield of low-strength classes (e.g. C18). Olsson and Oscarsson (2017) showed that for a large sample of Norway spruce from Sweden, Norway and Finland, an improved grading accuracy corresponding to the improvement of using  $IP_{E4E}$  rather than  $E_{a,12\%}$  defined herein, for prediction of bending strength, led to a doubling of the yield in high-strength classes like C35 and C40. Viguier et al. (2017) performed a study based on the same samples of Norway spruce and Douglas fir as those considered in the present study. They showed that the yield in class C30 increased with about 25% by using an IP that gave a similar accuracy as what  $IP_{E2E}$  defined herein does, rather than  $E_{a,12\%}$  for prediction of bending strength.

## 7 Conclusions

The main conclusions of the research are as follows:

- Results presented confirm that axial dynamic MoE give good prediction of bending strength for structural size timber of both Norway spruce (*P. abies*) and Douglas fir (*P. menziesii*) ( $R^2 = 0.58$  and  $R^2 = 0.47$ , respectively). Dynamic axial MoE is, however, a poor predictor of strength of narrow dimension boards of oak (*Q. robur* and *Q. petraea*) ( $R^2 = 0.22$ ). This was explained by the fact that knots and fibre distortion around knots in narrow dimension oak boards often affect the entire cross section, resulting in very low local stiffness and low strength. This is not captured by a measure of a global/average MoE of a board. Thus, dynamic axial MoE is not a suitable IP for prediction of strength of narrow dimension boards of oak.
- For Norway spruce (*P. abies*) and Douglas fir (*P. menziesii*), excellent prediction of bending strength can be obtained when an IP established on the basis of scanning of fibre orientation is used in combination with dynamic axial MoE. When based upon scanning of four sides, this IP ( $IP_{E4E}$ ) gave coefficients of determination to

bending strength as high as  $R^2 = 0.72$  and  $R^2 = 0.62$  for Norway spruce and Douglas fir, respectively. Results from earlier investigations on the relationship between coefficient of determination and yield in strength classes imply that the yield in high-strength class would increase by up to 50% if dynamic axial MoE is replaced by the best performing IP presented herein ( $IP_{E4E}$ ) for prediction of bending strength.

- Fibre orientation on oak (*Q. robur* and *Q. petraea*) surfaces can be determined by means of laser scanning, just as it can for surfaces of softwood species. Moreover, for oak just as for softwood species, IPs based on data of fibre orientation alone give good prediction of bending strength. When an IP based only on data from fibre orientation scanning of two wide faces ( $E_{b,90,nom,2-side}$ ) of narrow dimension boards of oak, a coefficient of determination to bending strength as high as  $R^2 = 0.56$  was obtained. This would be sufficient for commercial grading of narrow dimension boards of oak for use, e.g. as lamellae in engineered wood products like cross-laminated timber or glulam.

**Acknowledgements** We thank Robert Collet from Arts et Metiers who was the fundraiser and leader of the projects from which data was collected.

**Funding** The data used in this study was obtained thanks to several sources of funding: funding from the regional council of Bourgogne Franche-Comté and Carnot ARTS institute; funding from the French National Research Agency through the ANR CLAMEB project (ANR-11-RMNP-0015). The cooperation between the research teams was funded by Arts et Metiers.

**Data availability** The datasets generated during and/or analysed during the current study are not publicly available due to patented methods used for computations, but are available from the corresponding author on reasonable request.

## Compliance with ethical standards

**Conflict of interest** The authors declare that they have no conflict of interest.

## References

- ALSC (2014) List of approved machines. American Lumber Standard Committee, Germantown [http://www.alsc.org/untreated\\_machinegraded\\_mod.htm](http://www.alsc.org/untreated_machinegraded_mod.htm). Accessed 14 March 2018
- Bechtel FK (1985) Beam stiffness as a function of point-wise E, with application to machine stress rating. In: Proceedings of International Symposium on Forest Products Research, CSIR, Pretoria, South Africa. p 22–26
- Blass HJ, Gard W (1994) Machine strength grading of timber. In: Proceedings of the Pacific Timber Engineering Conference, Gold Coast, Australia, 11–15 July 1994



- Boughton G (1994) Superior sorting of timber using localized stiffness on edge. In: Proceedings of the Pacific Timber Engineering Conference, Gold Coast, Australia, 11–15 July 1994
- Brancheriau L, Paradis S, Baillères H (2007) Bing: beam identification by non-destructive grading (Cirad). <http://ur-biwooeb.cirad.fr/en/products/bing/what-is-it>. Accessed 6 September 2018. <https://doi.org/10.18167/62696E67>
- Corder SE (1965) Localized deflection related to bending strength of lumber. In: Proceedings of the Second Symposium on Nondestructive Testing of Wood, Spokane, WA, USA
- Daval V, Pot G, Belkacemi M, Meriaudeau F, Collet R (2015) Automatic measurement of wood fiber orientation and knot detection using an optical system based on heating conduction. *Opt Express* 23:33529–33539. <https://doi.org/10.1364/OE.23.033529>
- Dinwoodie JM (2000) Timber: its nature and behaviour. E & FN Spon. New Fetter Lane, London
- EN 13183-1 (2003+AC:2004) Moisture content of a piece of sawn timber—part 1: determination by oven dry method
- EN 14081-2 (2010+A1:2012) Timber structures—strength graded structural timber with rectangular cross section—part 2: machine grading: additional requirements for initial type testing
- EN 338 (2016) Structural timber—strength classes
- EN 384 (2016) Structural timber—determination of characteristic values of mechanical properties and densities
- EN 408 (2010+A1:2012) Timber structures—structural timber and glued laminated timber—determination of some physical and mechanical properties
- Epaud F (2007) De la charpente romane à la charpente gothique en Normandie (from roman to gothic carpentry in Normandy). Publications du CRAHM, Caen
- Faydi Y (2017) Mechanical grading of oak wood using vibrational and grain angle measurements. Doctoral dissertation, Arts et Métiers ParisTech, Cluny, France
- Faydi Y, Brancheriau L, Pot G, Collet R (2017) Prediction of oak wood mechanical properties based on the statistical exploitation of vibrational response. *BioResources* 12(3):5913–5927. <https://doi.org/10.15376/biores.12.3.5913-5927>
- Foschi RO (1987) A procedure for the determination of localized modulus of elasticity. *Holz Roh Werkst* 45:257–260
- Galligan WL, McDonald KA (2000) Machine grading of lumber—practical concerns for lumber producers. Forest Products Laboratory, General Technical Report FPL-GTR-7, Madison, WI, USA
- Görlacher R (1990) Klassifizierung von Brettschichtholzlamellen durch Messung von Longitudinalschwingungen (classification of glulam laminations by measurement of longitudinal vibrations). Dissertation. Versuchsanstalt für Stahl, Holz und Steine der Universität Fridericiana in Karlsruhe, Germany
- Guitard D (1987) Mécanique du matériau bois et composites (Mechanics of the wood material and composites). Cepadues, Toulouse
- Hanhijärvi A, Ranta-Maunus A (2008) Development of strength grading of timber using combined measurement techniques. Report of the Combigrade project—phase 2. VTT Publication 686
- Hatayama Y (1984) A new estimation of structural lumber considering the slope of the grain around knots. *Bulletin of the Forestry and Forest Products Research Institute, Japan*, 326:69–167
- Hoffmeyer P (ed.) (1995) Styrkesortering ger mervärde, Del 2 – Tillgängelig teknik (Strength grading adds value, Part 2 – Available technique). Laboratoriet for Byningsmaterialer, Danmarks Tekniske Universitet, Teknisk Rapport 335–1995, ISSN 0908–3871 (in Danish, Norwegian and Swedish)
- Hu M (2018) Studies on the fibre direction and local bending stiffness of Norway spruce timber. Doctoral dissertation, Linnaeus University, Växjö, Sweden
- IGN (2017) French National Forest Inventory. <http://inventaire-forestier.ign.fr/>. Accessed 20 Oct 2017
- Jehl A (2012) Modeling of lumber's mechanical behavior using x-rays densitometry and laser imaging. Doctoral dissertation, Arts et Métiers ParisTech, Cluny, France
- Kass AJ (1975) Middle ordinate method measures stiffness variation within pieces of lumber. *For Prod J* 25:33–41
- Kollman FFP, Côté WA (1968) Principles of wood science and technology. Springer Verlag, Berlin Heidelberg
- Lukacevic M, Füssl J, Eberhardsteiner J (2015) Discussion of common and new indicating properties for the strength grading of wooden boards. *Wood Sci Technol* 49:551–576. <https://doi.org/10.1007/s00226-015-0712-1>
- Matthews PC, Beech BH (1976) Method and apparatus for detecting timber defects. U.S. Patent 3976384
- NF EN 975-1 (2009) Sawn timber—appearance grading of hardwoods—part 1: Oak and beech. AFNOR, Paris
- Oh JK, Shim K, Kim KM, Lee JJ (2009) Quantification of knots in dimension lumber using a single-pass X-ray radiation. *J Wood Sci* 55:264–272. <https://doi.org/10.1007/s10086-009-1031-7>
- Ohlsson S, Perstorper M (1992) Elastic wood properties from dynamic tests and computer modeling. *J Struct Eng* 118:2677–2690. [https://doi.org/10.1061/\(ASCE\)0733-9445\(1992\)118:10\(2677\)](https://doi.org/10.1061/(ASCE)0733-9445(1992)118:10(2677))
- Olsson A (2016) Determination of sawn timber properties using laser scanning—development potentials and industrial applications. In: Proceedings of WCTE 2016, World Conference on Timber Engineering, Vienna, Austria, 22–25 August 2016
- Olsson A, Oscarsson J (2017) Strength grading on the basis of high resolution laser scanning and dynamic excitation: a full scale investigation of performance. *Eur J Wood Wood Prod* 75:17–31. <https://doi.org/10.1007/s00107-016-1102-6>
- Olsson A, Oscarsson J, Serrano E, Källsner B, Johansson M, Enquist B (2013) Prediction of timber bending strength and in-member cross-sectional stiffness variation on the basis of local wood fibre orientation. *Eur J Wood Wood Prod* 71:319–333. <https://doi.org/10.1007/s00107-013-0684-5>
- Oscarsson J, Olsson A, Enquist B (2014) Localized modulus of elasticity in timber and its significance for the accuracy of machine strength grading. *Wood Fiber Sci* 46:489–501
- Rellstab C, Bühler A, Graf R, Folly C, Gugerli F (2016) Using joint multivariate analyses of leaf morphology and molecular-genetic markers for taxon identification in three hybridizing European white oak species (*Quercus* spp.). *Ann For Sci* 73:669–679. <https://doi.org/10.1007/s13595-016-0552-7>
- Schlotzhauer P, Wilhelms F, Lux C, Bollmus S (2018) Comparisons of three systems for automatic grain angle determination on European hardwood for construction use. *Eur J Wood Wood Prod* 76:911–923. <https://doi.org/10.1007/s00107-018-1286-z>
- Schoch W, Heller I, Schweingruber FH, Kienast F (2004) Wood anatomy of central European species. <http://www.woodanatomy.ch>. Accessed 10 March 2018
- Stängle SM, Brüchert F, Heikkilä A, Usenius T, Usenius A, Sauter UA (2015) Potentially increased sawmill yield from hardwoods using X-ray computed tomography for knot detection. *Ann For Sci* 72:57–65. <https://doi.org/10.1007/s13595-014-0385-1>
- Viguier J (2015) Classement mécanique des bois de structure. Prise en compte des singularités dans la modélisation du comportement mécanique (Timber grading. Modeling of the mechanical behavior using defects). Doctoral dissertation, Université de Lorraine, France
- Viguier J, Jehl A, Collet R, Bléron L, Meriaudeau F (2015) Improving strength grading of timber by grain angle measurement and mechanical modeling. *Wood Mater Sci Eng* 10:145–156. <https://doi.org/10.1080/17480272.2014.951071>
- Viguier J, Bourreau D, Bocquet JF, Pot G, Bléron L, Lanvin JD (2017) Modelling mechanical properties of spruce and Douglas fir timber by means of X-ray and grain angle measurements for strength grading purpose. *Eur J Wood Wood Prod* 75:527–541. <https://doi.org/10.1007/s00107-016-1149-4>

WoodEye (2016) A method and device for evaluating a wooden board (Förfarande och anordning för utvärdering av en träplanka). European Patent EP 2 823 298 B1, 28 December 2016

Zhou J, Shen J (2003) Ellipse detection and phase demodulation for wood grain orientation measurement based on the tracheid effect. *Opt Lasers Eng* 39:73–89. [https://doi.org/10.1016/S0143-8166\(02\)00041-6](https://doi.org/10.1016/S0143-8166(02)00041-6)